Primary Frequency Control Contribution From Smart Loads Using Reactive Compensation

Zohaib Akhtar, *Student Member, IEEE*, Balarko Chaudhuri, *Senior Member, IEEE*, and Shu Yuen Ron Hui, *Fellow, IEEE*

***Abstract*—Frequency-dependent loads inherently contribute to primary frequency response. This paper describes additional contribution to primary frequency control based on voltage-dependent noncritical (NC) loads that can tolerate a wide variation of supply voltage. By using a series of reactive compensators to decouple the NC load from the mains to form a smart load (SL), the voltage, and hence the active power of the NC load, can be controlled to regulate the mains frequency. The scope of this paper focuses primarily on reactive compensators for which only the magnitude of the injected voltage could be controlled while maintaining the quadrature relationship between the current and voltage. New control guidelines are suggested. The effectiveness of the SLs in improving mains frequency regulation without considering frequency-dependent loads and with little relaxation in mains voltage tolerance is demonstrated in a case study on the IEEE 37 bus test distribution network. Sensitivity analysis is included to show the effectiveness and limitations of SLs for varying load power factors, proportion of SLs, and system strengths.**

***Index Terms*—Demand response (DR), demand-side management (DSM), electric spring (ES), primary frequency control, reactive compensator, smart load (SL), voltage control.**

I. Introduction

WITH GROWING penetration of asynchronous inverter-interfaced generation (e.g., wind, solar photovoltaic, etc.) the effective inertia of future power systems is expected to reduce drastically. This would cause unacceptably large excursions and rates of change of the system frequencies (RoCoF) following a loss of infeed which would threaten the system security [1]. Moreover, loss-of-infeeds larger than the reserve capacity of the system could be more likely for example, due to a cable fault within a dc grid. These would make the primary frequency control much more challenging than what it is now.

Manuscript received September 7, 2014; revised December 24, 2014; accepted February 6, 2015. This work was supported in part by the Commonwealth Scholarship Commission; by the Engineering and Physical Science Research Council, U.K., under Grant EP/K036327/1; by the University of Hong Kong Seed Funds under Seed Project 201111159239 and Project 201203159010; and by the Hong Kong Research Grant Council under Grant T23-701/14-N. Paper no. TSG-00898-2014.

Z. Akhtar and B. Chaudhuri are with the Department of Electrical and Electronic Engineering, Imperial College London, London SW7 2AZ, U.K. (e-mail: b.chaudhuri@imperial.ac.uk).

S. Y. R. Hui is with the Department of Electrical and Electronic Engineering, Imperial College London, London SW7 2AZ, U.K., and also with the Department of Electrical and Electronic Engineering, The University of Hong Kong, Hong Kong.

Color versions of one or more of the figures in this paper are available online at http://ieeexplore.ieee.org.

Digital Object Identifier 10.1109/TSG.2015.2402637

To overcome the problem, asynchronous generators like the wind farms and even some selected categories of loads (demand) would be required to contribute to frequency control alongside the conventional synchronous plants with fast ramp-rates and natural response of the frequency-dependant loads. Several papers have been published on contribution of wind farms on frequency control [2]–[4]. On the demand/load end, the focus has primarily been on load scheduling [5] and grid frequency control [6] through on/off control of loads which has been collectively referred to as "demand response" or "demand-side management (DSM)" [7]–[9]. As the loads are connected in parallel across the supply/mains, the easiest way to exercise any sizeable variation in their average power consumption is to operate them in on/off mode. Frequency control using variation in average power consumption of the loads is achieved by switching those on/off with appropriate duty cycles [10], [11]. This is also predicated on the fact that the potential candidate loads for DSM e.g., air conditioners, especially, the ones supplied through adjustable speed drives exhibit a constant power characteristics over a wide voltage range [12] which rules out any possibility of continuous control. Moreover, if the load is operating at its rated capacity, the average power consumption of the load can only be reduced, not increased through on/off control.

Different methods have been proposed for controlling voltage at different system nodes based on optimization of reactive power compensation [13]–[15]. The basic aim in all these methods is to control the system voltage within an allowable limit rather than controlling the frequency by manipulation of load. With certain types of voltage-dependant loads e.g., electric heating [16], lighting (especially, LED lighting [17]), small motors with no stalling problems (e.g., fans, ovens, dish washers, and dryers) [18], it is possible, in principle, to exercise a continuous variation in active power consumed by controlling the supply voltage [19]. However, it is neither straightforward (given the stiffness of even moderately weak systems) nor recommendable (as there are sensitive loads connected to the mains which require tightly regulated voltage) to vary the supply/mains voltage. Therefore, these loads would have to be decoupled from the supply/mains through a voltage compensator.

The concept of smart load (SL) using electric springs (ES) was proposed in [20] as a mean of exercising continuous control of both voltage and frequency in an unified framework. A SL comprises of a voltage compensator (ES) connected in series between the supply/mains and a voltage-dependant load

which can tolerate a wider variation in supply voltage. Such a load is henceforth referred to as NC load. By controlling the voltage injected by the compensator, the mains voltage can be regulated while allowing the voltage (and hence the power) across the NC load to be controlled. Thus, a SL ensures a tightly regulated voltage across the other sensitive loads connected to the mains, while varying its own power consumption and thus, contribute to system frequency control. In fact, both the mains voltage and frequency can be simultaneously regulated if the magnitude and phase angle (with respect to the current) of the voltage injected by the compensator is controlled. However, injection of voltage at any arbitrary phase angle other than $\pm 90°$ would require exchange of active power and hence an additional storage element or a back-to-back converter arrangement.

Since the initial proof-of-concept using a SL with a ES, a number of papers have been published on this topic focusing on dynamic modeling [21], performance analysis [22], [23] and control [24], [25] of ES for voltage regulation and power quality improvement [26] only including a comparison of voltage control using ES against static compensator (STATCOM) [27]. In particular, the results in [27] suggest that the use of SLs has the potential of using only a fraction of the total reactive power required by a STATCOM to achieve similar or better voltage regulation than a STATCOM in the distribution network. The change of voltage control paradigm from a centralized one using STATCOM to a distributed one based on SLs deserves more investigation, especially on the aspects of better control and total reactive power requirements.

In this paper, the contribution of the SLs with reactive compensation to primary frequency control is illustrated for the first time. In [21]–[27] the active and/or reactive power of the SL has been controlled implicitly by controlling the active and/or reactive power of the series connected compensator using appropriate limits [27] which is not necessarily the best strategy. Ultimately, it is the net change in active and/or reactive power of the overall SL which affects the voltage or frequency regulation. Therefore, an improved control philosophy is reported in this paper to directly modify the active power consumption of the SL. Any power electronic compensator used for control of active power will either provide reactive or active or both active and reactive compensations. The latter two would require an energy storage or a back-to-back converter arrangement. Reactive only compensation is preferable from that point of view and was therefore, considered as a first option in this paper.

The focus of this paper is restricted to SLs based on reactive (Q) compensation (SLQ) and impedance-type loads only. This implies that the compensator in series with the impedance-type NC load can inject a voltage of controllable (within acceptable bounds) magnitude but only in quadrature (either leading or lagging) with respect to the current. As there is only one control variable, the magnitude of the voltage, such as SLQ can be controlled either to control the mains voltage or the frequency, but not both at the same time. It is shown that a SLQ operated in frequency control mode can contribute to primary frequency control for both under- and over-frequency events for nonunity power factor loads with little (<10%) relaxation in voltage tolerance of the NC load. Frequency regulation is achieved at the expense of slight deterioration in supply voltage regulation which still remains well within the acceptable limits for a range of system strengths. The effectiveness of a SLQ is demonstrated through a case study on the IEEE 37 bus test system. The frequency and voltage regulation and the total reactive capacity of the compensators required for different load power factors, proportion of SLs, and system strength are also compared through a rigorous sensitivity study. The limitations of the SLQ are explained highlighting the possible need for a SL based on active (P) and reactive (Q) compensation (SLPQ) [22] to achieve both distributed voltage and primary frequency control simultaneously.

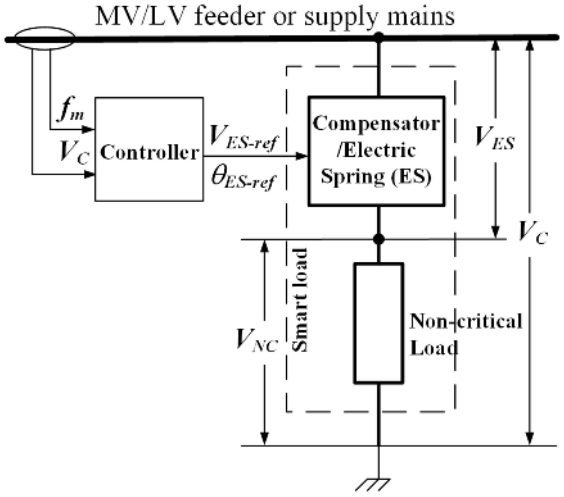

Fig. 1. SL configuration.

II. Smart Load (SL) With Reactive Compensation (SLQ)

A. Basic Principle

Demand or loads could be categorized into two types: 1) critical; or 2) sensitive loads, which require a tightly regulated supply voltage and NC loads which can tolerate a wider fluctuation in supply voltage without causing perceivable disruption to the consumers. Some of these NC loads, e.g., air-conditioners draw a constant power from the supply over a wide range of voltage. Others, e.g., water/space heater, lighting systems (especially, LEDs), small motors (e.g., in fans, ovens, dishwashers, and dryers) consume power according to their terminal voltages. Such voltage-dependent NC loads are candidates for SLs.

A SL is formed by inserting a voltage compensator (or ES) in series between the supply/mains and the load itself as shown in Fig. 1.

By controlling the injected voltage (V_{ES}), the voltage across the NC load (V_{NC}) and hence, its power consumption can be controlled. Collective action of many such SLs could contribute to regulating the frequency of the mains. At times of generation shortfall (excess), the voltage across the NC loads is

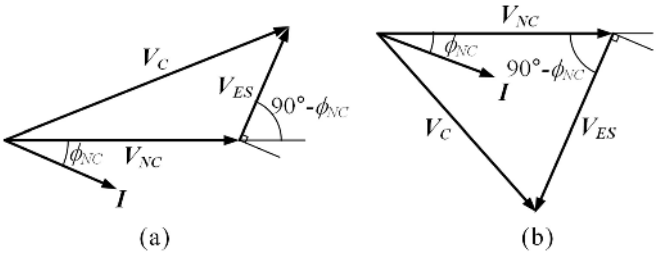

Fig. 2. Phasor schematic for SLQ. (a) For inductive compensation mode. (b) For capacitive compensation mode.

reduced (increased). The "controller" block is described later in Section II-C.

Depending on the type of compensation used, there could be two types of SLs. For a SLQ, the voltage injected by the compensator has to be in phase quadrature with the current. This implies only the magnitude of the injected voltage can be controlled while maintaining the phase angle at ±90°. On the other hand, a SL with both active and reactive compensation (SLPQ) does not have any restriction on the phase angle. Hence, both the magnitude and phase angle of the voltage injected by the compensator can be controlled independently. This allows control of both active and reactive power of the SL, enabling voltage, and frequency regulation at the same time. However, energy storage (e.g., battery or super-capacitor) or a back-to-back converter arrangement is required by the compensator to support the active power exchanged. The scope of this paper is restricted to SLQ only. Henceforth, the term SL would represent a SLQ unless otherwise specified.

Power losses will be incurred due to the flow of load current through the converter even under normal condition when the ES is not producing any compensation. This is similar to the power losses incurred in any power electronic interface (e.g., drive circuit) of the loads. Notably, ES with only one converter will incur less loss than a typical drive circuit with back-to-back converters. Alternatively, special arrangements could be made to bypass the converter or leave it under a floating state under normal condition through use of hybrid (mechanical-electronic) switching.

In this paper, simple impedance-type load representation is used for the NC loads. Frequency dependance of the loads is neglected to isolate the contribution to primary frequency response from voltage dependance alone. As most impedance-type loads (including those in the study system used later in this paper) are of resistive-inductive (R-L) nature, the discussion throughout the rest of this paper assumes R-L-type loads only. However, the inferences are general and are applicable to resistive-capacitive loads as well.

For a R-L-type SLQ, the phasor diagrams are shown in Fig. 2 for (a) inductive and (b) capacitive compensation modes. From the phasor diagrams, the relationship between the voltages across the compensator/ES (V_{ES}), the NC load (V_{NC}) and the mains (V_C) can be expressed as

$$V_C^2 = V_{\mathrm{NC}}^2 + V_{\mathrm{ES}}^2 \pm 2V_{\mathrm{NC}}V_{\mathrm{ES}}\sin\phi_{\mathrm{NC}}. \tag{1}$$

The positive and negative sign corresponds to the inductive and capacitive compensation modes, respectively. Using $V_{\mathrm{NC}} = I \times Z_{\mathrm{NC}}$, the compensator voltage (V_{ES}) in inductive compensation mode can be expressed in terms of the current (I) and supply/mains voltage (V_C) as

$$V_{\mathrm{ES}} = -IZ_{\mathrm{NC}}\sin\phi_{\mathrm{NC}} \pm \sqrt{V_C^2 - (IZ_{\mathrm{NC}}\cos\phi_{\mathrm{NC}})^2} \tag{2}$$

$$= -F(I, V_C). \tag{3}$$

While in capacitive compensation mode, V_{ES} can be expressed in terms of the current (I) and supply/mains voltage (V_C) as

$$V_{\mathrm{ES}} = +IZ_{\mathrm{NC}}\sin\phi_{\mathrm{NC}} \pm \sqrt{V_C^2 - (IZ_{\mathrm{NC}}\cos\phi_{\mathrm{NC}})^2} \tag{4}$$

$$= +F(I, V_C). \tag{5}$$

It can be seen that in inductive compensation mode, there is only one possible value for V_{ES} corresponding to a value of I and V_C as the second root of (2) will always be fictitious (negative). However, it is possible to have two values of V_{ES} corresponding to a value of I and V_C in capacitive compensation mode (4). The relationship between I and V_{ES} is used later in Section II-C in the control loop for a SLQ.

B. Analysis of Active and Reactive Power Capabilities

It is important to estimate active and reactive power capabilities of the SL to evaluate its effectiveness in frequency and voltage control. This section provides new information about such capabilities related to primary frequency control and the boundaries of operation under different power factors. The analysis leads to new guidance for the use of the SLs for primary frequency control. For a constant supply voltage V_C, the voltage across the NC load V_{NC} can be written as a function of the compensator voltage V_{ES} (1). It can be used to calculate the change in active (ΔP_{SL}) and reactive (ΔQ_{SL}) power of the SL for different values of V_{ES} considering both phase angles (±90°). The corresponding values of the reactive compensation required (Q_{ES}) and the NC load voltage (V_{NC}) can also be determined.

The reactive compensation Q_{ES} required to change the active and reactive power of a SLQ rated at 1 p.u. is shown in Fig. 3 for three different power factors of the NC load. The dotted lines represent the original curves without any restriction on the magnitude of V_{NC}, while the solid lines represent the region in which V_{NC} is limited within the range of 0.8–1.2 p.u. The supply voltage (V_C) is considered to be tightly regulated at 1 p.u. It can be seen from Fig. 3(b) that for unity power factor (green trace) there are no positive values of ΔP_{SL}. This implies that a SLQ with unity power factor can only be used in an under-frequency event as the voltage across the NC load cannot exceed 1.0 p.u. Decreasing ΔP_{SL} will result in some nonzero value of ΔQ_{SL} which would impact the supply voltage depending on the system strength.

Both positive and negative values of ΔP_{SL} can be achieved for loads with nonunity power factors as shown by the blue and black traces in Fig. 3(b). So a SLQ with nonunity power factor loads can provide frequency control for both under-frequency and over-frequency events. From Fig. 3(c), it is evident that for SLQs with power factor 0.9 lagging, ΔP_{SL} is positive only when the compensator is in capacitive mode ($Q_{\mathrm{ES}} < 0$).

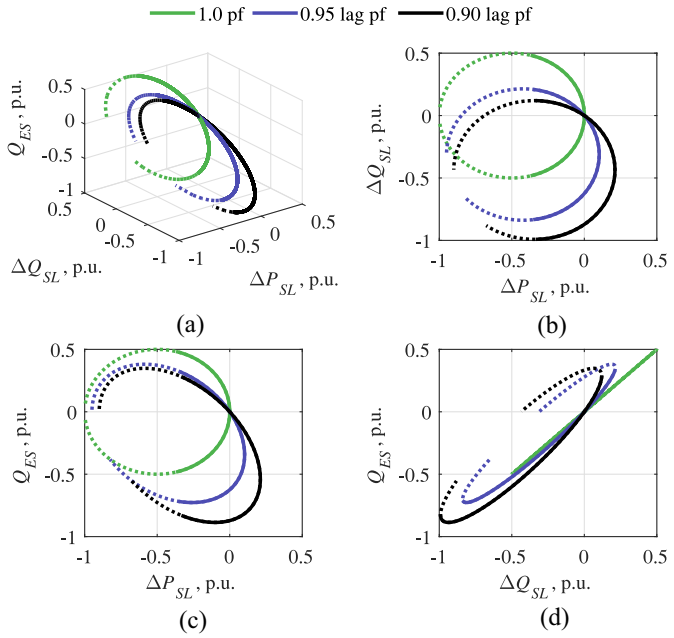

Fig. 3. (a) Reactive compensation required (z-axis) to change active (x-axis) and reactive (y-axis) power of a SL for different power factors. (b) X-Y view. (c) X-Z view. (d) Y-Z view.

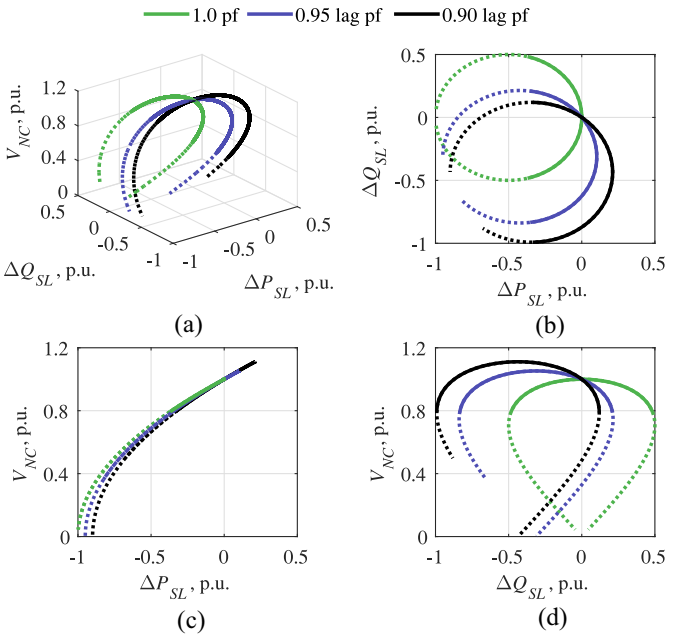

Fig. 4. (a) Voltage across the NC load required (z-axis) to change active (x-axis) and reactive (y-axis) power of a SL for different power factors. (b) X-Y view. (c) X-Z view. (d) Y-Z view.

This is due to the fact that the voltage across the NC load can be higher than supply voltage of 1.0 p.u. only when the compensator is in the capacitive mode [Fig. 2(b)]. Hence, the phase angle of the controller is set at $-90°$ for an over-frequency event in case of a R-L-type NC load. There can be two possible values of $V_{\rm ES}$ to achieve the same value of $\Delta P_{\rm SL}$. The smaller value should be considered to ensure minimum rating of the compensator.

The change in SL reactive power ($\Delta Q_{\rm SL}$) is negative when $\Delta P_{\rm SL} > 0$. This would increase the supply voltage and hence, the active power consumption of other voltage-dependent loads connected to the mains resulting in an improved frequency regulation. The maximum positive value of $\Delta P_{\rm SL}$ occur at the point when the inductive reactive power of the NC load is exactly matched by the capacitive reactive power of the ES. The current flowing though the SLQ is maximum at this point. $\Delta P_{\rm SL}$ cannot be increased beyond this point as any increase in $V_{\rm ES}$ will result in a decrease in the SL current.

In case of an under-frequency event, with a 0.9 lagging power factor load, the compensator can either be in inductive or capacitive mode [Fig. 3(b) and (c)]. However, the $Q_{\rm ES}$ required in inductive mode is lower than that required in the capacitive mode for the same value of $\Delta P_{\rm SL}$. Hence, the phase angle of the compensator is set at $+90°$. This would reduce the supply voltage and hence, the active power consumed by other voltage-dependant loads connected to the supply/mains. If there is no restriction on $V_{\rm NC}$, the current flowing though the SL can be reduced to zero by injecting a voltage $V_{\rm ES}$ equal to V_C. Hence, the minimum possible value of $\Delta P_{\rm SL}$ will be equal to negative of the nominal value of active power consumed by the SL under normal conditions. However, the minimum allowed value of $V_{\rm NC}$ will determine the minimum value of $\Delta P_{\rm SL}$ that can be achieved.

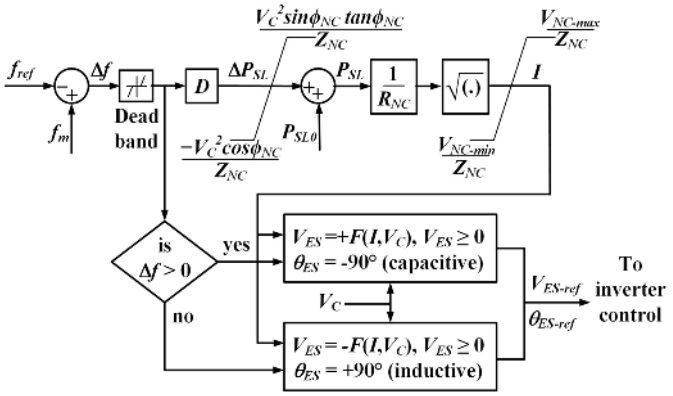

Fig. 5. Control loop for frequency regulation using R-L-type SLQ.

Fig. 4 shows the voltage across the NC load required to change the active and reactive power of the SLQ (1 p.u.). It is clear that $V_{\rm NC}$ can not be greater than 1.0 p.u. for a unity power factor load. The operating regions on these curves can be restricted according to the maximum allowable variations in the NC load voltage. A simple way of enforcing that is to limit the minimum and maximum current for a given NC load impedance as shown later in Section II-C.

C. Control of SLs

The control objective is to vary the active power consumption of the SL within the capability of the SLQ in order to regulate the supply frequency. Variation in active power is achieved by controlling the magnitude of the voltage injected by the compensator (or ES) which causes the voltage across the NC load to vary within the acceptable limits. The control loop is shown in Fig. 5.

An ideal phase-lock-loop (PLL) was assumed for frequency measurement. Any difference (Δf) between the reference (f_{ref}) and measured (f_m) frequency is filtered through a dead band (± 0.01 Hz) and multiplied by a droop gain $D = (0.215/P_{\text{SL0}})$ to calculate the required change in active power (ΔP_{SL}) consumed by the SL about its nominal value (P_{SL0}). The value of ΔP_{SL} is limited based on the maximum and minimum possible values calculated from the supply voltage (V_C), and the NC load impedance ($Z_{\text{NC}} \angle \phi_{\text{NC}}$). The active power to be consumed by the SL at a given instant (P_{SL}) is obtained by adding up the nominal power (P_{SL0}) and the desired change (ΔP_{SL}).

As the compensator exchanges only reactive power, the current (I) through the SL is obtained by calculating square root of P_{SL} divided by R_{NC}. The current magnitude is limited based on the acceptable limits ($V_{\text{NC-max}} - V_{\text{NC-min}}$) on the voltage across the NC load using its impedance (Z_{NC}).

From I, the magnitude of the injected voltage (V_{ES}) can be derived using (3) and (5). The phase angle of the injected voltage (θ_{ES}) would be set according to the sign of Δf as shown in Fig. 5. Capacitive compensation ($\theta_{\text{ES}} = -90°$) reduces P_{SL} while an inductive compensation ($\theta_{\text{ES}} = +90°$) is more effective in increasing P_{SL} as explained earlier in Section II-B. An additional benefit is that inductive (capacitive) compensation decreases (increases) the supply/mains voltage slightly which would result in decrease (increase) in power consumption of other voltage-dependent loads connected to the mains which helps the frequency regulation further.

To determine the magnitude of V_{ES}, the corresponding positive and real solution(s) of (3) and (5) are considered. If there are multiple positive real solutions, the minimum value of V_{ES} is selected to ensure minimum reactive capacity ($Q_{\text{ES}} = V_{\text{ES}} \times I$) of the compensator/ES. The reference values of the voltage magnitude (V_{ES}) and the phase angle (θ_{ES}) are provided to the standard control system of the inverter. An ideal tracking response is assumed for the inverters so that the reference values of the compensator voltage ($V_{\text{ES-ref}}, \theta_{\text{ES-ref}}$) are the same as their actual ($V_{\text{ES}}, \theta_{\text{ES}}$) values. For a practical inverter, we will have to consider the nonideal behavior of the PLL, the time delay for the inverter control, and dynamics of the dc link which might cause the phase angle to change a little from the reference angle ($\pm 90°$) in transient state to account for the losses in the inverter.

III. Case Study

A case study is set up based on the following considerations: the supply frequency is a global variable which is influenced by the combined action of several generators and loads connected at the bulk power transmission and distribution networks, respectively. It is not straightforward to conduct simulation studies with detailed representation of both bulk power transmission network and low- or medium-voltage (LV/MV) distribution network. Hence, aggregated representation of the LV/MV networks as lumped loads is commonly used for frequency control studies. As the SLs would be deployed at the LV/MV level within the distribution network, aggregated representation of LV/MV networks as loads would not be adequate. Therefore, a two-part bottom-up and top-down approach

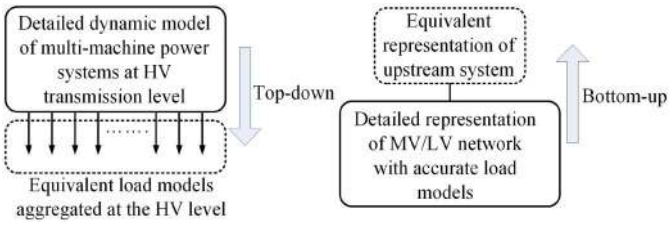

Fig. 6. Top-down and bottom-up approaches for system modeling.

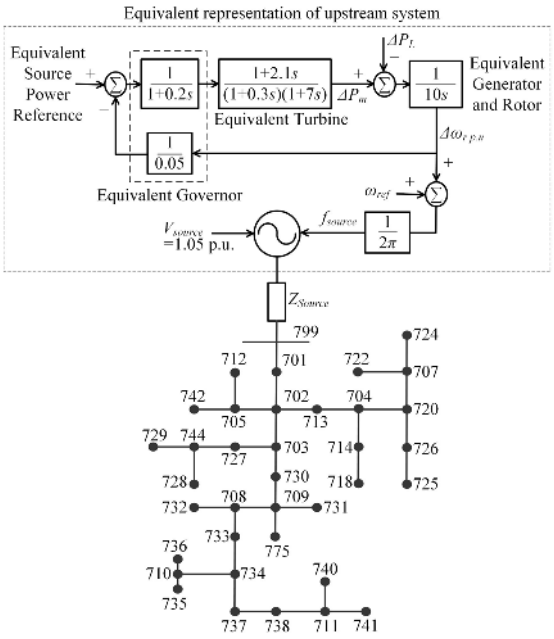

Fig. 7. IEEE 37-bus test system with equivalent dynamic representation of the upstream system at bus 799.

as shown in Fig. 6 has been adopted for this research. In this paper, results of the simulation studies with detailed representation of a distribution network is presented with an equivalent model of the upstream system (bottom-up approach) with same capacity as the load capacity. In a follow-up paper, similar results with a detailed representation of the bulk power transmission network (including dynamic models of generators, etc.) and aggregated loads would be presented to complement the results presented in this paper (top-down approach).

As a standard distribution system, the IEEE 37-bus test system, shown in Fig. 7 is considered for this paper. It is a three-phase medium voltage radial distribution system with both single phase and unbalanced three phase loads. There are 32 static loads with a mix of constant impedance (Z), constant current (I), and constant power (P) i.e., ZIP characteristics. About 50% of these loads are considered as noncritical [27] and assumed to be of purely impedance type while the other loads (connected to the supply/mains) are represented by the ZIP model. The location of SLs is the same as the location of original loads in the standard system. The actual percentage of the voltage dependent NC load is the key to the effectiveness of SLs. Also, the limits of voltage variations allowable across different loads would differ widely which affects the above percentage. The results of the sensitivity analysis in

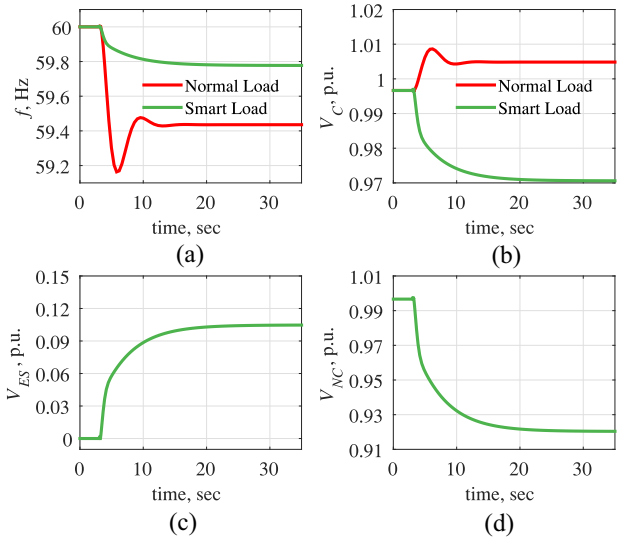

Fig. 8. Dynamic variation of (a) supply frequency, (b) supply voltage at bus 738, (c) voltage across NC load, and (d) voltage injected by compenastor/ES following an under-frequency event at $t = 2.0$ s.

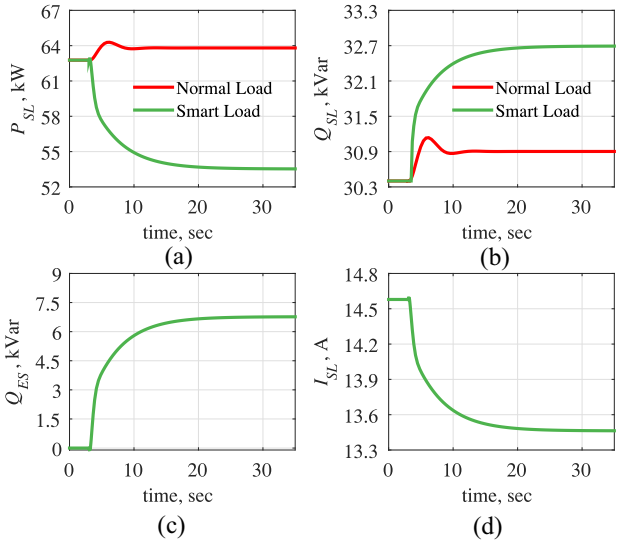

Fig. 9. Dynamic variation of (a) active power, (b) reactive power consumed by the SL, (c) reactive compensation, and (d) current following an under-frequency event at $t = 2.0$ s.

Section V show the effect of larger (and smaller) percentage of NC loads.

In order to have comparison of the proposed technique with load control by variation of the supply voltage, model of a standard STATCOM was developed as a current source capable of injecting inductive or capacitive reactive power in the system, in case of a under-/over-frequency event. To have a fair comparison with SLQs, distributed STATCOMs were considered to be connected in parallel with all SLs.

The upstream system is connected at bus 799 and modeled as a variable frequency voltage source with appropriate P-f droop and time-constants as in [28] to mimic the typical power-frequency variation of the grid. A variable series impedance is used to simulate the upstream network of varying strengths.

IV. Simulation Results

Time domain simulations have been carried out in MATLAB SIMULINK using a time step of 20 μs. Frequency disturbances were created by applying 15% step changes in the equivalent source power reference. Simulation results at bus 738 are shown here separately for under- (Figs. 8 and 9) and over-frequency (Figs. 10 and 11) events. It is a bus close to the far end of the distribution system. So the voltage regulation at this bus is relatively poor compared to the buses close to the upstream system. A small increase in voltage is observed for a reduction in the supply frequency. This is due to decrease in network reactance with a decrease in the frequency. Similarly, an increase in frequency results in a slight decrease in voltage due to an increase in network reactance. There are no frequency dependant loads in the standard IEEE 37 test feeder.

In both cases (Figs. 8 and 10), the SL ensures much improved frequency regulation compared to a normal load (i.e., a NC load without a series compensator/ES). The mains voltage regulation turns out to be slightly worse but still staying

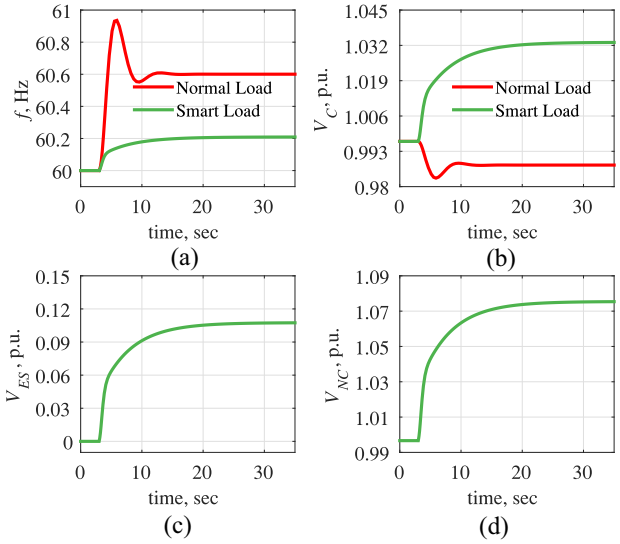

Fig. 10. Dynamic variation of (a) supply frequency, (b) supply voltage at bus 738, (c) voltage across NC load, and (d) voltage injected by compenastor/ES following an over-frequency event at $t = 2.0$ s.

well within the acceptable (5%) limits. In this case, the compensator is required to inject about 10% of the rated voltage while the variation in voltage across the NC load is limited to $\pm$10%. This transient voltage variation will not cause perceivable change in the performance of NC loads like heating [16], lighting (especially, LED lighting [17]), and small motors with no stalling problems (e.g., fans, ovens, dish washers, dryers) [18]. With normal loads (red traces), the mains voltage would increase (decrease) in the under- (over-) frequency case which aggravates the situation resulting in the poor frequency regulation.

The change in active/reactive power of the SL and the reactive compensation required is shown in Figs. 9 and 11 for under- and over-frequency events, respectively. A change

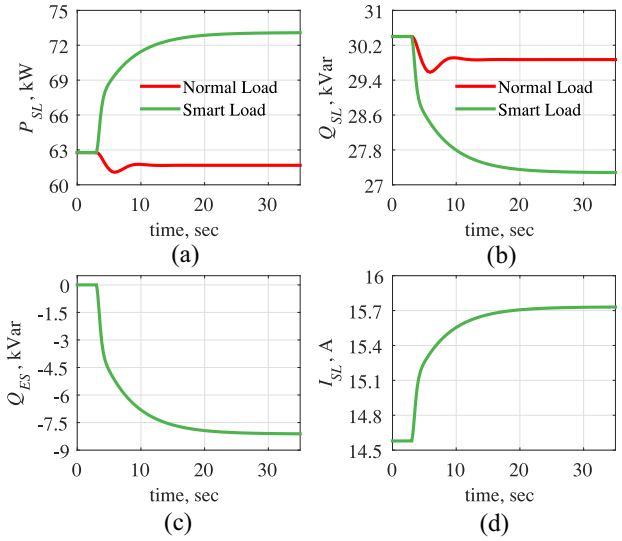

Fig. 11. Dynamic variation of (a) active power, (b) reactive power consumed by the SL, (c) reactive compensation, and (d) current following an over-frequency event at $t = 2.0$ s.

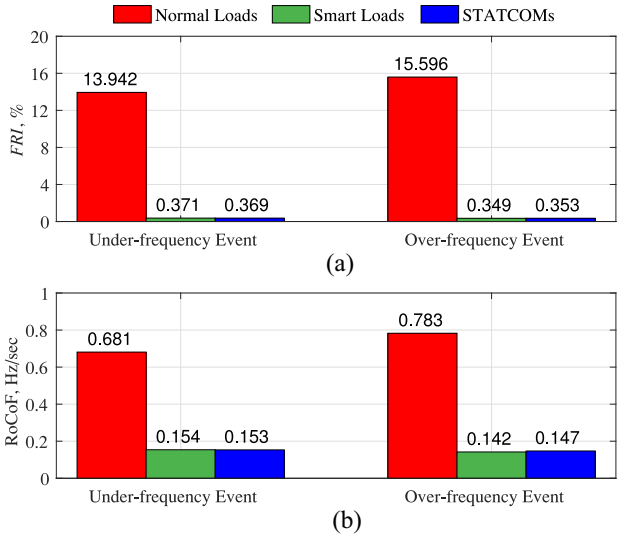

Fig. 12. (a) FRI (7) and (b) average RoCoF for under- and over-frequency events.

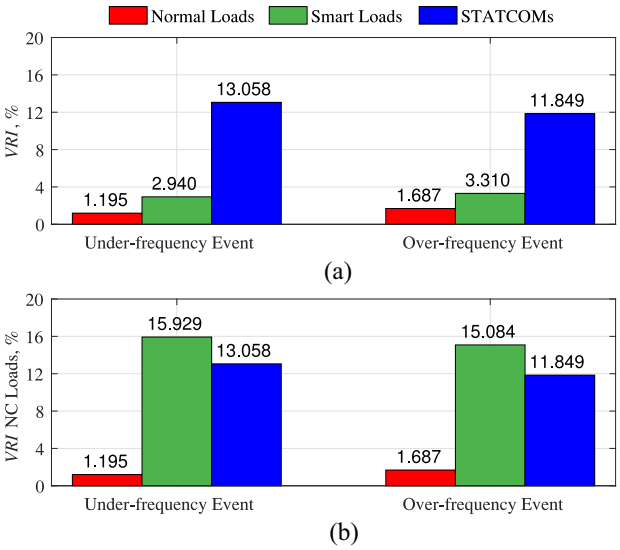

Fig. 13. (a) VRI (6) across the supply/mains and (b) NC load for under- and over-frequency events.

of 10 kW in active power consumption of the SL could be achieved with less than 8 kvar reactive compensation.

After presenting the time-domain responses at a particular bus (bus 738), the collective performance of all the SLs is captured through system-wide averaged measures like voltage regulation index (VRI) and frequency regulation index (FRI). VRI is defined as

$$\text{VRI(in \%)} = \frac{\sum_{i=1}^{N_{\text{bus}}} \left\{ \max_t |V_i(t) - V_{\text{ref}}| \times W_{vi} \right\}}{N_{\text{bus}}} \times 100 \qquad (6)$$

where

$$\begin{aligned} W_{vi} &= 1 \text{ if } \max_t |V_i(t) - V_{\text{ref}}| \leq 0.05 \text{ p.u.} \\ &= 2 \text{ if } 0.05 \text{ p.u.} < \max_t |V_i(t) - V_{\text{ref}}| \leq 0.1 \text{ p.u.} \\ &= 10 \text{ if } \max_t |V_i(t) - V_{\text{ref}}| > 0.1 \text{ p.u.} \end{aligned}$$

In the above expression, $V_i(t)$ is the p.u. value of voltage at the ith bus as a function of time, V_{ref} is the reference voltage in p.u., N_{bus} is the total number of buses, and W_{Vi} is a weighted penalty factor to impose extra penalty if the voltage variation is outside the allowed range. The maximum deviation from reference value over time for each bus is considered. Similarly, FRI is defined as

$$\text{FRI(in \%)} = \frac{\sum_{i=1}^{N_{\text{bus}}} \left\{ \max_t |f_i(t) - f_{\text{ref}}| \times W_{fi} \right\}}{N_{\text{bus}}} \times 100 \qquad (7)$$

where

$$\begin{aligned} W_{fi} &= 1 \text{ if } \max_t |f_i(t) - f_{\text{ref}}| \leq 0.5 \text{ Hz} \\ &= 10 \text{ if } \max_t |f_i(t) - f_{\text{ref}}| > 0.5 \text{ Hz} \end{aligned}$$

where $f_i(t)$ is the p.u. value of frequency at the ith bus as a function of time, f_{ref} is the reference frequency in p.u., N_{bus} is the total number of buses, and W_{fi} is a weighted penalty factor.

The RoCoF is also very important for normal operation of sensitive loads. It is defined as the maximum value calculated over a moving window of 500 ms.

It can be seen from Fig. 12 that both FRI and RoCoF have improved significantly with the SLs for both under- and over-frequency events. A similar performance in terms of frequency control is achieved by using STATCOMs.

Fig. 13(a) shows that the VRI for the mains has got worse with SLs.

All the node voltages remained within the allowable (5%) limits. Improvement in frequency regulation is achieved through a wider variation in voltage (and hence power) across the NC load as shown in Fig. 13(b). Nonetheless, this variation was limited to less than 10% which can be tolerated in short-term by most NC loads. The VRI for STATCOMs is very large compared to that for SLs. STATCOMs achieve frequency

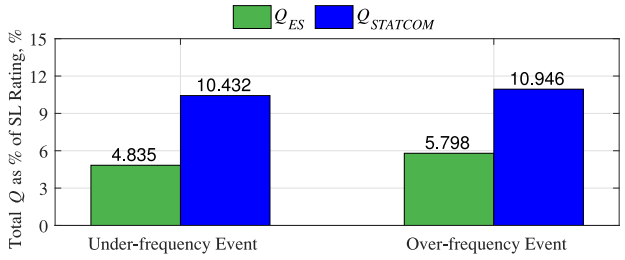

Fig. 14. Total reactive capacity of the compensators/ESs and STATCOMs expressed as a percentage of the SL rating.

regulation by varying the supply voltage. Most node voltages violated the allowable (5%) limits which would affect the critical loads. As the STATCOMs change the supply voltage, the value of VRI for NC loads is same as that for supply voltage [Fig. 13(b)]. However, it can be seen that VRI for NC loads is higher in case of SLs compared to STATCOMs. This is due to the fact that the NC loads share larger burden of voltage variation to safeguard the critical loads.

The total reactive capacity required for all the compensators/ESs and STATCOMs is expressed as a percentage of the total SL apparent power (kVA) rating and is shown in Fig. 14.

In this case, the above frequency regulation performance could be achieved with reactive compensation which is only a fraction (less than 6%) of the total SL capacity. This is encouraging from a size and cost point of view. It can be seen that the STATCOMs required nearly twice as much reactive power compared to the SLs for achieving a similar frequency regulation. This is due to the fact that changing supply voltage requires more reactive power than controlling the voltage across the NC loads (which are decoupled from the supply through the compensator) even for moderately stiff systems.

V. Sensitivity Studies

The performance of the SL depends on several factors including the load power factor, proportion of SL present in the system, system strength, etc. The results presented in Section IV assumes a particular value for these factors as described earlier in Section III. However, the values of these factors could be different which calls for a sensitivity study. Due to space restrictions, the results of the sensitivity studies are presented only for under-frequency events.

The effect of variation in load (R-L-type) power factor is shown in Fig. 15. Similar frequency regulation [FRI in Fig. 15(a)] below 0.37% is achieved over a range of power factor values. However, the supply voltage regulation [VRI in Fig. 15(b)] gets worse with increasing values of power factor. Above 0.95 (lagging) power factor, the voltage regulation for most nodes is outside the acceptable (5%) limit which causes an increase in the slope due to a larger penalty factor. The deterioration in voltage regulation can be explained from Fig. 3(b). In order to achieve a certain value of ΔP_{SL} (along the negative direction for under-frequency events), the change in ΔQ_{SL} is more for increasing (lagging) power factor. Thus, voltage regulation is worse for power factors closer to unity.

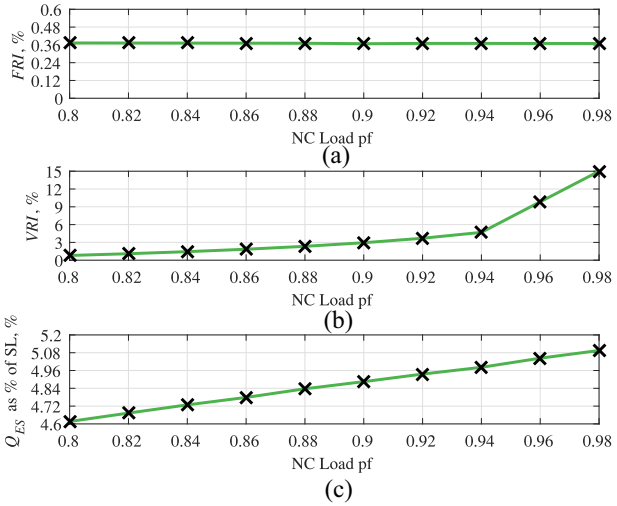

Fig. 15. Impact of load power factor on (a) FRI (7), (b) VRI (6) for mains and NC load, and (c) total reactive capacity of the compensators/ESs expressed as a percentage of the SL rating.

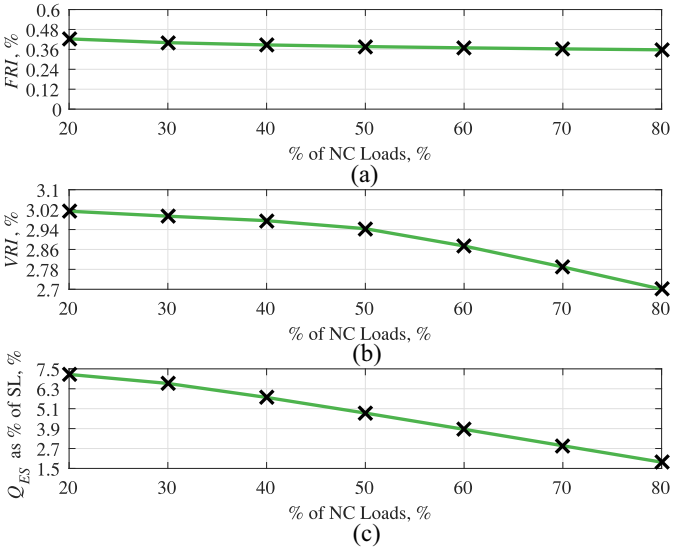

Fig. 16. Impact of proportion of SL on (a) FRI (7), (b) VRI (6) for mains and NC load, and (c) total reactive capacity of the compensators/ESs expressed as a percentage of the SL rating.

From Fig. 3(c), it is clear that the reactive compensation (Q_{ES}) required to achieve a certain value of ΔP_{SL} (along the negative direction for under-frequency events) is higher for increasing power factor (lagging) of the loads. This is reflected in the trend of (Q_{ES}) in Fig. 15(c).

In Fig. 16, the effect of varying the proportion of NC/SL over a range of 20% to 80% is shown.

As before, very similar FRI [Fig. 16(a)] around 0.371% could be achieved over the whole range. With higher proportion of SLs, the supply voltage regulation [Fig. 15(b)] is improved due to lesser impact of each SL on ΔQ_{SL} and hence, the supply voltage V_C.

In order to analyze the effect of the system strength, the value of impedance in series with the power source (representing the upstream system) is varied between 0% and 200% of the nominal value. Fig. 17 shows that similar FRI

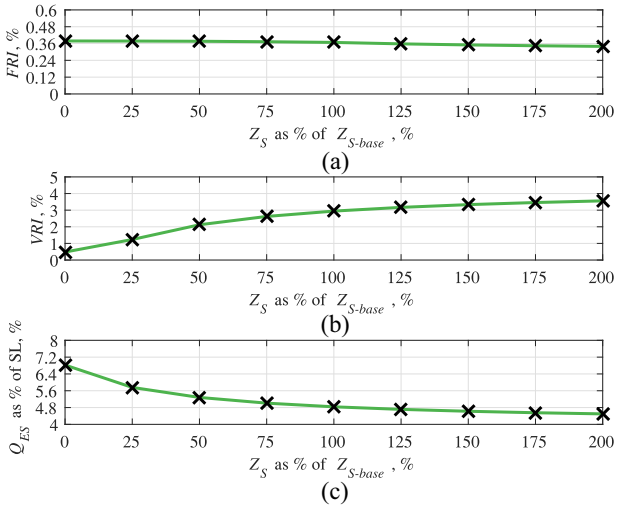

Fig. 17. Impact of system strength on (a) FRI (7), (b) VRI (6) for mains and NC load, and (c) total reactive capacity of the compensators/ESs expressed as a percentage of the SL rating.

[Fig. 17(a)] below 0.371% could be achieved for different system strengths but at the expense of poorer voltage regulation [Fig. 17(b)] for weaker (higher source impedance) systems which is as expected.

The reactive compensation (Q_{ES}) required [Fig. 17(c)] is less for weaker systems. This is due to larger contribution to change in active power consumption from the other loads connected to the supply (as explained earlier in Section II-B) due to larger variation in supply voltage in the case of weaker systems.

This paper shows that the rating of the reactive compensator is limited to less than 10% of the load rating. Thus, for a 2.0 kW water heater, a 200 var compensator would be required which would cost about $4–6. This is assuming $ 20–30/kvar for reactive compensation at LV/MV levels which should be less than that ($ 55–70/kvar) at the bulk power compensation (range of MVar or above) level [29]. The voltage variation across NC loads was limited to 10% which can be tolerated by small motors, heating and lighting (especially, LED) loads for tens of seconds. Of course, these figures depend on several factors (some of which has been considered in the sensitivity analysis) and further investigations are required to ascertain these.

VI. Conclusion

The effectiveness and limitations of SLs in terms of their contribution to primary frequency control is presented in this paper. Without considering any primary frequency response contribution from frequency dependence of loads, the SLs on their own are shown to achieve much improved frequency regulation with little relaxation in voltage tolerance for the NC loads and a small (fraction of the load rating) reactive compensation. With SL using reactive compensation only (SLQ), the mains voltage regulation got slightly worse (still staying well within acceptable limits). If tighter voltage regulation is a requirement due to presence of sensitive loads, then SLs with both active and reactive compensation (SLPQ) would have to be used to enable simultaneous control of both frequency and voltage—this would be reported in a follow-on paper. Sensitivity analysis is presented to show the effectiveness of the SLQs under varying load power factors, proportion of SLs and system strengths.

Two important practical considerations toward realizing SLs are: 1) the rating (which dictates the cost and size) of the reactive compensator and 2) the range of variation in voltage across the NC load connected in series with the compensator. This paper shows that the rating of the reactive compensator is limited to less than 10% of the load rating. The range of voltage variation can be limited to 10% without any perceivable impact on the consumers.

Control of load power consumption through voltage variation using a shunt reactive compensation device like STATCOM will require more reactive power as it will be more difficult to change the system voltage compared to the voltage across the NC load. Also it will result in a poor voltage profile for all other loads including the critical loads.

In this paper, simple impedance-type representation is assumed for the SLs while a mix of constant current, constant power, and impedance-type characteristics is used for the other loads connected to the mains. Frequency dependance of loads are neglected to isolate the impact on primary frequency response from the voltage-dependant part alone which leads to pessimistic results. Frequency dependence of loads and typical P-V, Q-V sensitivities of specific types of candidate SLs would have to be incorporated in future for more realistic results.

References

[1] G. Stein. (2011). *Frequency Response Technical Sub-Group Report, National Grid*. [Online]. Available: http://www.nationalgrid.com/NR/rdonlyres/2AFD4C05-E169-4636-BF02-EDC67F80F9C2/50090/FRTSGGroupReportFinal.pdf

[2] I. Erlich and M. Wilch, "Primary frequency control by wind turbines," in *Proc. IEEE Power Energy Soc. Gen. Meeting*, Minneapolis, MN, USA, Jul. 2010, pp. 1–8.

[3] Y. G. Rebours, D. S. Kirschen, M. Trotignon, and S. Rossignol, "A survey of frequency and voltage control ancillary services part I: Technical features," *IEEE Trans. Power Syst.*, vol. 22, no. 1, pp. 350–357, Feb. 2007.

[4] H. T. Ma and B. H. Chowdhury, "Working towards frequency regulation with wind plants: Combined control approaches," *IET Renew. Power Gener.*, vol. 4, no. 4, pp. 308–316, Jul. 2010.

[5] A. H. Mohsenian-Rad, V. W. S. Wong, J. Jatskevich, R. Schober, and A. Leon-Garcia, "Autonomous demand-side management based on game-theoretic energy consumption scheduling for the future smart grid," *IEEE Trans. Smart Grid*, vol. 1, no. 3, pp. 320–331, Dec. 2010.

[6] J. A. Short, D. G. Infield, and L. L. Freris, "Stabilization of grid frequency through dynamic demand control," *IEEE Trans. Power Syst.*, vol. 22, no. 3, pp. 1284–1293, Aug. 2007.

[7] P. Palensky and D. Dietrich, "Demand side management: Demand response, intelligent energy systems, and smart loads," *IEEE Trans. Ind. Informat.*, vol. 7, no. 3, pp. 381–388, Aug. 2011.

[8] M. Parvania and M. Fotuhi-Firuzabad, "Demand response scheduling by stochastic SCUC," *IEEE Trans. Smart Grid*, vol. 1, no. 1, pp. 89–98, Jun. 2010.

[9] M. A. A. Pedrasa, T. D. Spooner, and I. F. MacGill, "Scheduling of demand side resources using binary particle swarm optimization," *IEEE Trans. Power Syst.*, vol. 24, no. 3, pp. 1173–1181, Aug. 2009.

[10] K. Samarakoon, J. Ekanayake, and N. Jenkins, "Investigation of domestic load control to provide primary frequency response using smart meters," *IEEE Trans. Smart Grid*, vol. 3, no. 1, pp. 282–292, Mar. 2012.

[11] W. Gu *et al.*, "Adaptive decentralized under-frequency load shedding for islanded smart distribution networks," *IEEE Trans. Sustain. Energy*, vol. 5, no. 3, pp. 886–895, Jul. 2014.

[12] K. Tomiyama, J. P. Daniel, and S. Ihara, "Modeling air conditioner load for power system studies," *IEEE Trans. Power Syst.*, vol. 13, no. 2, pp. 414–421, May 1998.
[13] K. Christakou, D.-C. Tomozei, J.-Y. Le Boudec, and M. Paolone, "GECN: Primary voltage control for active distribution networks via real-time demand-response," *IEEE Trans. Smart Grid*, vol. 5, no. 2, pp. 622–631, Mar. 2014.
[14] L. Liu, H. Li, Y. Xue, and W. Liu, "Reactive power compensation and optimization strategy for grid-interactive cascaded photovoltaic systems," *IEEE Trans. Power Electron.*, vol. 30, no. 1, pp. 188–202, Jan. 2015.
[15] C.-H. Liu and Y.-Y. Hsu, "Design of a self-tuning PI controller for a STATCOM using particle swarm optimization," *IEEE Trans. Ind. Electron.*, vol. 57, no. 2, pp. 702–715, Feb. 2010.
[16] S. Wong and S. Pelland, "Demand response potential of water heaters to mitigate minimum generation conditions," in *Proc. IEEE Power Energy Soc. Gen. Meeting (PES)*, Vancouver, BC, Canada, Jul. 2013, pp. 1–5.
[17] C. K. Lee, S. Li, and S. Y. R. Hui, "A design methodology for smart LED lighting systems powered by weakly regulated renewable power grids," *IEEE Trans. Smart Grid*, vol. 2, no. 3, pp. 548–554, Sep. 2011.
[18] N. Lu, Y. Xie, Z. Huang, F. Puyleart, and S. Yang, "Load component database of household appliances and small office equipment," in *Proc. IEEE Power Energy Soc. Gen. Meeting*, Pittsburgh, PA, USA, Jul. 2008, pp. 1–5.
[19] C. K. Lee, K. L. Cheng, and W. M. Ng, "Load characterisation of electric spring," in *Proc. IEEE Energy Conv. Cong. Expo. (ECCE)*, Denver, CO, USA, Sep. 2013, pp. 4665–4670.
[20] S. Y. R. Hui, C. K. Lee, and F. F. Wu, "Electric springs—A new smart grid technology," *IEEE Trans. Smart Grid*, vol. 3, no. 3, pp. 1552–1561, Sep. 2012.
[21] N. R. Chaudhuri, C. K. Lee, B. Chaudhuri, and S. Y. R. Hui, "Dynamic modeling of electric springs," *IEEE Trans. Smart Grid*, vol. 5, no. 5, pp. 2450–2458, Sep. 2014.
[22] S. C. Tan, C. K. Lee, and S. Y. R. Hui, "General steady-state analysis and control principle of electric springs with active and reactive power compensations," *IEEE Trans. Power Electron.*, vol. 28, no. 8, pp. 3958–3969, Aug. 2013.
[23] C. K. Lee and S. Y. R. Hui, "Reduction of energy storage requirements in future smart grid using electric springs," *IEEE Trans. Smart Grid*, vol. 4, no. 3, pp. 1282–1288, Sep. 2013.
[24] C. K. Lee, N. R. Chaudhuri, B. Chaudhuri, and S. Y. R. Hui, "Droop control of distributed electric springs for stabilizing future power grid," *IEEE Trans. Smart Grid*, vol. 4, no. 3, pp. 1558–1566, Sep. 2013.
[25] C. K. Lee, B. Chaudhuri, and S. Y. R. Hui, "Hardware and control implementation of electric springs for stabilizing future smart grid with intermittent renewable energy sources," *IEEE J. Emerg. Sel. Topics Power Electron.*, vol. 1, no. 1, pp. 18–27, Mar. 2013.
[26] Y. Shuo, S. C. Tan, C. K. Lee, and S. Y. R. Hui, "Electric spring for power quality improvement," in *Proc. IEEE Appl. Power Electron. Conf. Expo. (APEC)*, Fort Worth, TX, USA, Mar. 2014, pp. 2140–2147.
[27] X. Luo *et al.*, "Distributed voltage control with electric springs: Comparison with STATCOM," *IEEE Trans. Smart Grid*, vol. 6, no. 1, pp. 209–219, Jan. 2015.
[28] P. Kundur, N. J. Balu, and M. G. Lauby, *Power System Stability and Control*. vol. 7. New York, NY, USA: McGraw-Hill, 1994,
[29] J. Kueck, B. Kirby, T. Rizy, F. Li, and N. Fall, "Reactive power from distributed energy," *Elect. J.*, vol. 19, no. 10, pp. 27–38, Dec. 2006.

Zohaib Akhtar (S'14) received the B.Sc. (Hons.) and M.Sc. degrees in electrical engineering from the University of Engineering and Technology, Lahore, Pakistan, in 2008 and 2011, respectively. He is currently pursuing the Ph.D. degree from Imperial College London, London, U.K.

His current research interests include renewable energy, power distribution, and smart grids.

Balarko Chaudhuri (M'06–SM'06) received the Ph.D. degree in electrical and electronic engineering from Imperial College London, London, U.K., in 2005.

He is currently a Senior Lecturer with the Control and Power Research Group, Imperial College London. His current research interests include electric power transmission systems, control theory, smart grids, and renewable energy.

Dr. Chaudhuri is an Associate Editor of the IEEE SYSTEMS JOURNAL and *Control Engineering Practice*. He is a member of the Institution of Engineering and Technology (IET) and Conseil International des Grands Réseaux Électriques (International Council on Large Electric Systems).

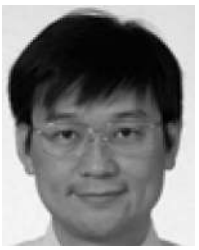

Shu Yuen Ron Hui (M'87–SM'94–F'03) received the B.Sc. (Hons.) degree in electrical and electronic engineering from the University of Birmingham, Birmingham, U.K., in 1984, and the D.I.C. and Ph.D. degrees in electrical engineering from Imperial College London, London, U.K., in 1987.

Since 2010, he has been a Part-Time Chair Professor at Power Electronics, Imperial College London. He is currently the Philip Wong Wilson Wong Chair Professor with the University of Hong Kong, Hong Kong. He has published over 200 technical papers, including about 170 refereed journal publications and book chapters. He holds over 55 patents, which have been adopted by the industry.

Prof. Hui was the recipient of the IEEE Rudolf Chope Research and Development Award from the IEEE Industrial Electronics Society, the IET Achievement Medal (Crompton Medal) from the Institution of Engineering and Technology in 2010, and the 2015 IEEE William E. Newell Power Electronics Award. He is an Associate Editor of the IEEE TRANSACTIONS ON POWER ELECTRONICS and the IEEE TRANSACTIONS ON INDUSTRIAL ELECTRONICS. He is a Fellow of the Australian Academy of Technological Sciences and Engineering.